Electrical Power and Energy Systems 169 (2025) 110792

Contents lists available at ScienceDirect

International Journal of Electrical Power and Energy Systems

journal homepage: www.elsevier.com/locate/ijepes

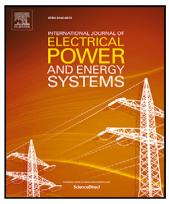

Corrective soft bus-bar splitting for reliable operation of hybrid AC/DC grids

Basel Morsy [a,b,*], Matthew Deakin [c], Adolfo Anta [a], Jochen Cremer [b]

[a] Austrian Institute of Technology AIT GmbH, Giefinggasse 4, Vienna, 1210, Austria
[b] TU Delft, Mekelweg 5, Delft, 2628 CD, Netherlands
[c] Newcastle University, Newcastle upon Tyne, NE1 7RU, United Kingdom

ARTICLE INFO

Keywords:
Hybrid AC/DC grids
Network topology reconfiguration
Corrective switching
Congestion management

ABSTRACT

Transmission system operators face significant hurdles in integrating variable renewables and facilitating operational flexibility. This has sparked renewed interest in optimizing network capacity utilization. This paper explores the synergy between two flexibility-enhancing methods in hybrid AC/DC grids: Voltage Source Converter (VSC) set-point control pre- and post-contingency, and corrective Network Topology Reconfiguration (NTR). This paper introduces soft bus-bar splitting for converter substations with modular architectures to maximize grid flexibility. We propose an approach to optimize the topology of hybrid AC/DC grids under N-1 security constraints. As the original problem is NP-hard, this paper utilizes a column-and-constraint generation algorithm. Case studies on IEEE 5, 24, 39, and 67 hybrid AC/DC systems show superiority of the proposed method, manifested as significant improvement in operating costs, security, and converter redispatch needs, under different loading conditions.

1. Introduction

Decarbonization has manifested itself as an imperative necessity due to the climate crisis. The European Union's 2050 long-term goal is to become climate-neutral [1]. To achieve this goal, an energy transition away from fossil fueled energy sources and towards sustainable renewables has to be realized. In areas such as Northwest Europe, there is potential for hundreds of gigawatts of offshore wind capacity, among other areas of untapped renewable energy potentials. The integration of renewable energy sources comes with inherent variability and uncertainty due to the intermittent nature of renewable energy. Moreover, renewable energy sources are usually far away from load centers, which requires transport of energy over long distances. With the current situation of aging grids, growing demand, and more frequent extreme weather events, transmission system operators (TSOs) are required to improve grid flexibility and responsiveness to faults, imbalances, and congestion. The cost of congestion management in the EU during 2023 amounted to EUR 4 billion [2]. While a 2018 position paper by ENTSO-e reported inadequate reliability of the HVDC infrastructure [3]. To overcome these issues, TSOs have to pursue measures to maximize network utilization and capacity. To this end, there are two complementary directions forward: addressing infrastructural inadequacy via expansion, and addressing operational inefficiency by improving computation methods of controlling the available resources. The former includes the integration of direct current (DC) grid elements to create hybrid AC/DC grids, while the latter includes network topology reconfiguration (NTR) to enhance system security and mitigate congestion through rerouting of power flows. We discuss advancements in both directions in greater detail in the forthcoming subsections.

1.1. Hybrid AC/DC grids

The expansion of the existing transmission infrastructure is inevitable. While transmission networks are still predominantly alternative current (AC) grids, there has been many advocates for high voltage direct current (HVDC) technology; as it is becoming a more viable option to provide transmission where AC technologies are not cost-effective, or to improve controllability [4–6]. Fig. 1 shows HVDC connections in Europe. It is evident that hybrid AC/DC grids will be part of the future as technical obstacles (pointed out in [3] for example) are lifted by the recent advancements in power electronics-based technologies [7]. In this direction, large batteries, despite their high cost, are also starting to be deployed in strategic nodes to address congestion issues [8]. Voltage source converter (VSC)-based HVDC technologies are a key enabling technology of hybrid AC/DC transmission grids. Ref. [9] presents modeling formulations for optimal power flow (OPF) in the context of hybrid AC/DC grid. Particular focus has been given on the use of dynamic converter control (i.e., the use of post-contingency converter redispatch) as a corrective measure that can avoid costly

* Corresponding author at: Austrian Institute of Technology AIT GmbH, Giefinggasse 4, Vienna, 1210, Austria.
E-mail address: basel.morsy@ait.ac.at (B. Morsy).

https://doi.org/10.1016/j.ijepes.2025.110792
Received 27 January 2025; Received in revised form 15 April 2025; Accepted 25 May 2025
Available online 13 June 2025

Nomenclature

Parameters

B_l	Susceptance of line l.
a_{lk}	Status (faulty or not) of line l at state k.
a_{ck}^{conv}	Status of converter c at state k.
P_d	Demand at node d.
$\overline{P}_l$	Maximum capacity of line l.
C_g	Cost of dispatch for generator g.
C^{LS}	Cost of load shedding.
C^{curt}	Cost of curtailment.
$M_l^{\mathcal{E}}, M_l^{\delta}$	Big-M constants for line l used in disjunctive constraints related with power-flow/phase-angle limits.

Sets and Indices

$\mathcal{N}$	Set of all buses.
$\mathcal{N}^{aux}$	Set of auxiliary buses in all substations.
$\mathcal{K}$	Pre- and post-contingency states ($k = 0$ means pre-contingency).
$\mathcal{G}$	Set of all generators. Indexed by g.
$\mathcal{D}$	Set of all loads. Indexed by d.
$\mathcal{L}$	Set of original (non-auxiliary) lines. Indexed by l.
$\mathcal{L}^{DC}$	Set of DC lines. Indexed by l.
$\mathcal{C}$	Set of all converters. Indexed by c and refers to a single converter module. Subscript i is used to refer to the subset connected to node i.
$\mathcal{P}$	Set of all modular converter. Indexed by p and refers to a bulk converter that consists of a collection of converter modules.
$\mathcal{E}^r$	Set of auxiliary reconfiguration (switchable) lines in all substations. Subscript i is used to refer to the subset in substation i.
$\mathcal{E}^c$	Set of auxiliary coupler (switchable) lines in all substations. Subscript i is used to refer to the subset in substation i.
$\mathcal{K}^{(j)}$	Subset of contingencies considered at the jth iteration of C&CG method.
f_l	Origin node index of line l.
t_l	Terminal node index of line l.
m_i^p	Index of the ith module of bulk converter p.

Variables

P_g	Output power of generator g.
P_{gk}^{curt}	Power curtailed of generator g at contingency k
P_{lk}	Power flow in line l at contingency k.
δ_{ik}	Voltage phase angle of bus i at contingency k.
z_{lk}^r	Switching status of substation reconfiguration auxiliary line l at contingency k.
z_{lk}^c	Switching status of bus-bar coupler l at contingency k.
P_{dk}^{LS}	Load shedding at node d at contingency k.
UB, LB	Upper and lower bounds for the total cost.
ϕ_k	Total operating cost at contingency k.
Γ	Worst contingency cost.
P_{ck}^{DC}	Power injected at the DC side of converter c at contingency k.
P_{ck}^{AC}	Power injected at the AC side of converter c at contingency k.
γ_{pk}	Modular capacity allocation of bulk converter p at contingency k.

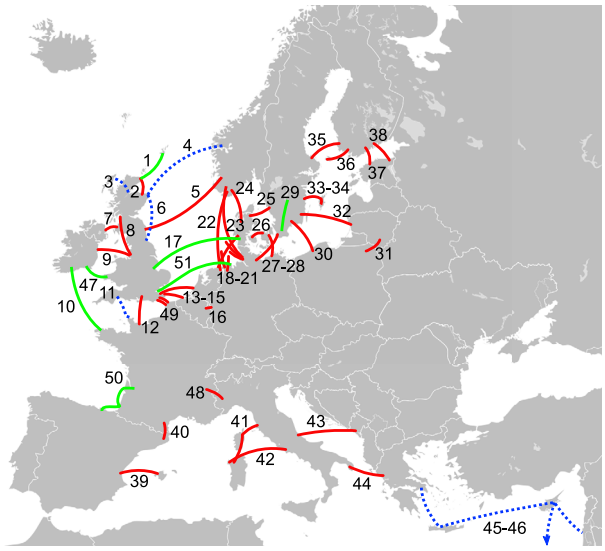

Fig. 1. HVDC connections in Europe [12]. Existing Planned Under construction.

generator redispatch to achieve N-1 security in hybrid AC/DC grids [10,11].

1.2. Network topology reconfiguration

NTR is an under-utilized source of flexibility and security enhancement. NTR can be in the form of transmission switching, or substation reconfiguration and bus-bar splitting (also referred to as substation switching). NTR helps in rerouting power flows in the grid via changing the topology. This is particularly useful in AC grids where power flows are not fully controllable. NTR has been investigated since the 1980s [13–15]. A mixed-integer linear programming (MILP) formulation of optimal transmission switching (OTS) was introduced in [16], which was extended in [17] to include N-1 security constraints. Ref. [18] addresses N-1 security constrained generation unit commitment with co-optimization of transmission switching. Ref. [19] addresses the security constrained unit commitment problem (SCUC) with preventive-corrective transmission switching. [20] presents a heuristic approach for pre-screening best transmission switching candidates. [21] addresses preventive security constrained optimal power flow (SCOPF) with transmission switching and substation reconfiguration, utilizing the full capability of NTR in one problem. The substation reconfiguration model proposed in this paper is based on [22]. [23] uses NTR with the objective being relieving congestion and hence reducing cost. [24] addresses SCOPF with substation reconfiguration and bus-bar splitting where the power flow model is based on injection shift factors. [25] shows that post-contingency busbar splitting could be vital to system security.

1.3. State-of-the-art and research gap

Recent studies address the potential benefit of using NTR in the context of hybrid AC/DC grids. Ref. [26] utilizes transmission switching and dynamic line rating to solve OPF. The proposed method is based on

using deep-learning to achieve real-time switching. Ref. [27] addresses the utilization of NTR in hybrid AC/DC distribution networks. [28] proposes a mixed-integer non-linear program (MINLP) formulation for NTR in hybrid AC/DC transmission grids. Convex relaxations are also introduced including second-order cone (SOC) relaxation, quadratic convex (QC) relaxation, and linear programming approximation (LPAC). [29] proposes a method for critical node identification and performing bus-bar splitting in hybrid AC/DC grids.

HVDC links and offshore wind collection systems usually connect to the AC transmission network at a substation via a monolithic modular multilevel converter (MMC) architecture acting as the AC/DC converter. Physically, an HVDC converter station with a shared DC bus but with multiple AC outputs could be constructed from parallel VSC converter modules. Some HVDC outlook literature discusses future use of standardized HVDC converter blocks (from which such a converter might be constructed) [30]. These standardized HVDC converter blocks allow for modular operation and provide extra controllability.

Switching problems are known to be NP-hard [31]. N-1 SCOPF with NTR can be intractable as the solution space grows exponentially with the system size. We identify two main sources of complexity in switching problems in general in the context of SCOPF: (i) the number of binary variables introduced, which depends on the number of substations considered for reconfiguration, (ii) the number of contingencies monitored, which depends on the size of the system. Decomposition methods can be used to address this computational complexity. Previous works show that there can exist a minimal subset of all contingency states that, when considered, the N-1 security constraints can be satisfied. This concept is known as umbrella contingencies [32, 33]. Using column-and-constraint generation (C&CG) algorithm that was originally introduced in [34] for robust optimization, the umbrella contingencies can be identified by solving a master problem and a subproblem iteratively.

The current state-of-the-art for using NTR in hybrid AC/DC grids clearly shows the potential of the use case. However, we identify a gap in the following aspects:

1. Converters can be used in a modular fashion. When applied in conjunction with NTR (namely bus-bar splitting), additional degrees of freedom can be exploited.
2. Security and reliability of operation have not been addressed adequately. NTR can be used as a corrective measure for security enhancement.
3. Modeling NTR leads to NP-hard optimization problems. Efficient algorithms are needed to address this computational complexity.

1.4. Paper contribution

1. We propose a novel approach to make ultimate use of converters with modular architectures via a so-called soft bus-bar splitting. The proposed approach results in optimizing the allocated converter capacity at each bus-bar section in the AC-side of converter substations.
2. We formulate the problem using a MILP model as a N-1 SCOPF in hybrid AC/DC grids. The proposed model utilizes network topology reconfiguration (NTR) and dynamic converter control (DCC) to provide both preventive and corrective actions in order to minimize operating costs and enhance security. We consider AC transmission line contingencies as well as VSC converter contingencies.
3. We utilize column-and-constraint generation algorithm to address the problem's inherent computational complexity.

To the best of our knowledge, the interaction between NTR and DCC with soft bus-bar splitting in hybrid AC/DC grids has not been studied before.

The rest of the paper is organized as follows. Mathematical models are presented in Section 2. Case studies are presented and discussed in Sections 3 and 4 respectively. Section 5 concludes.

2. Mathematical modeling

2.1. Substation switching model

To model substation switching (reconfiguration and bus-bar splitting), we use the so-called Augmented Network Representation (ANR) introduced in [35]. We consider substations with two bus-bar sections. A substation can be modeled via ANR as follows:

1. All grid components connected to the substation (e.g, transmission lines, generators, etc..) are assigned an auxiliary bus (illustrated in blue in Fig. 2).
2. The two sections of the substation's bus-bar are connected through a bus-bar coupler. The coupler is modeled as a switchable auxiliary line (coupler line) and is used to model splitting/merging actions.
3. Each auxiliary bus is connected to the two sections of the substation via switchable auxiliary lines (reconfiguration lines). A grid component can only be connected to one bus-bar section at any time.
4. Auxiliary lines have zero impedance as in practice these switches have very small impedance values. Such small values introduce numerical instabilities and ill-conditioning for the solver. Auxiliary lines are also assumed to have high capacity (modeled here at least as high as all the capacities of connected grid components) to allow for power flow in any direction between the two bus-bar sections.

Substation reconfiguration is the action of assigning grid components (connected to the substation in question) to bus-bar sections. Bus-bar splitting/merging is the action of switching off/on the bus-bar coupler. The two actions can take place pre- and/or post-contingency. We denote pre-contingency switching actions as *preventive* switching, while post-contingency switching is denoted as *corrective*. In this work we assume that substation reconfiguration is done preventively, while bus-bar splitting is exercised as a corrective action. Thus, the network topology is effectively unchanged in pre-contingency state as without splitting (switching off the bus-bar coupler) the substation is effectively one electrical node. This assumption aligns with the industry practices, where TSOs tend to operate the transmission grid with all the available redundancies and only perform switching actions upon contingencies or seasonally; in both cases switching actions are based on experience rather than a systematic optimal calculation.

In this work, we consider linear physics of the grid based on the DCOPF approximation. We formulate the problem as security constrained optimal power flow problem (SCOPF). Substation reconfiguration constraints can be written as:

$$\left\{ z^r_{lk} \in \{0,1\}, \quad \forall l \in \mathcal{E}^r \right. \tag{1a}$$

$$\sum_{l \in \mathcal{E}^r_i} z^r_{lk} = 1, \quad \forall i \in \mathcal{N}^{aux} \tag{1b}$$

$$|\delta_{f_l k} - \delta_{t_l k}| \leq (1 - z^r_{lk}) M^{\delta}_l, \quad \forall l \in \mathcal{E}^r \tag{1c}$$

$$\left. \begin{aligned} |P_{lk}| \leq z^r_{lk} M^{\mathcal{E}}_l, \quad \forall l \in \mathcal{E}^r \end{aligned} \right\}, \forall k \in \mathcal{K} \tag{1d}$$

$$z^r_{lk} = z^r_{l0}, \quad \forall l \in \mathcal{E}^r \; \forall k \in \mathcal{K} \setminus \{0\} \tag{1e}$$

where constraint (1b) ensures that each auxiliary bus is connected to only one auxiliary line (mutual exclusivity) to avoid circular flows inside the substation. Constraint (1c) ensures that the phase difference between an auxiliary bus and a section is zero if the auxiliary bus is connected to that section, otherwise the upper bound of the phase difference is set to M^{δ}_l to ensure that the phase angles of the bus-bar sections do not deviate too far from each other. Constraint (1d) models the capacity of auxiliary lines, where if the auxiliary line is

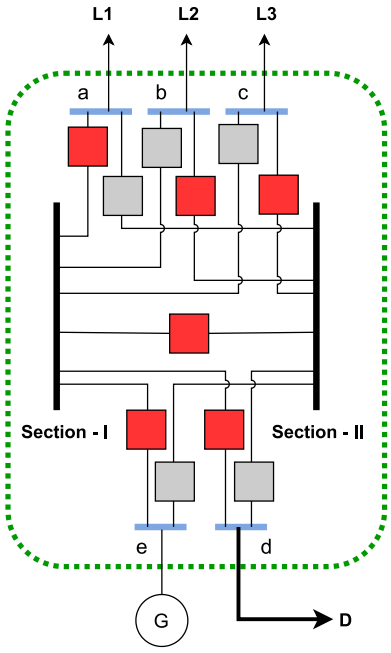

Fig. 2. Example of augmented network representation of a substation (enclosed by a dashed rectangle). switched on auxiliary line switched off auxiliary line auxiliary bus.

switched off, the capacity becomes zero, otherwise a sufficiently large upper bound for the power flow across an auxiliary line is set to $M_l^{\mathcal{E}}$. Finally, constraint (1e) enforces that all substation configurations post-contingency are the same as pre-contingency, which means that substation reconfiguration is done preventively.

Bus-bar splitting constraints are:

$$\left\{ z_{lk}^c \in \{0,1\}, \quad \forall l \in \mathcal{E}^c \right. \tag{2a}$$

$$|\delta_{f_l k} - \delta_{t_l k}| \leq (1 - z_{lk}^c) M_l^{\delta}, \quad \forall l \in \mathcal{E}^c \tag{2b}$$

$$\left. |P_{lk}| \leq z_{lk}^c M_l^{\mathcal{E}}, \quad \forall l \in \mathcal{E}^c \right\}, \forall k \in \mathcal{K} \tag{2c}$$

$$z_{l0}^c = 1, \forall l \in \mathcal{E}^c \tag{2d}$$

where constraint (2b) ensures that if the substation is not split, then the substation is regarded as a single electrical node with one phase angle, otherwise the two bus-bar sections of the substation have an upper bound for the phase angle difference. Constraint (2c) models the capacity of bus-bar couplers. Whereas constraint (2d) enforces all bus-bar couplers to be switched on in pre-contingency state ($k = 0$) so that splitting is only allowed as a corrective action.

2.2. DC grid model

We adopt a linear lossless model for the DC grid. The power flow equations become a network flow and can be written as:

$$\left\{ \sum_{\forall c \in C_i} P_{ck}^{DC} = \sum_{\forall l \in \mathcal{L}^{DC} | f_l = i} P_{lk} - \sum_{\forall l \in \mathcal{L}^{DC} | t_l = i} P_{lk}, \right.$$
$$\forall i \in \mathcal{N}^{DC} \tag{3a}$$

$$P_{lk}^{fr} + P_{lk}^{to} = 0, \quad \forall l \in \mathcal{L}^{DC} \tag{3b}$$

$$|P_{lk}| \leq \overline{P_l}, \quad \forall l \in \mathcal{L}^{DC} \tag{3c}$$

$$P_{ck}^{AC} + P_{ck}^{DC} = 0, \quad \forall c \in \mathcal{C} \tag{3d}$$

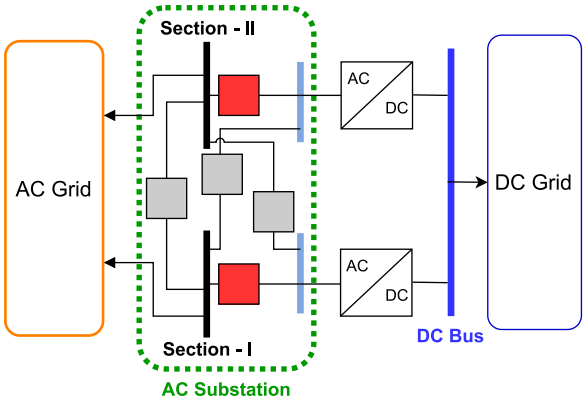

Fig. 3. Modular converter substation in augmented network representation exhibiting soft bus-bar splitting. switched on auxiliary line switched off auxiliary line auxiliary bus ⟶ Connections to the rest of the grid.

$$\left. |P_{ck}^{AC}|, |P_{ck}^{DC}| \leq a_{ck}^{conv} \overline{P_c}, \quad \forall c \in \mathcal{C} \right\}, \forall k \in \mathcal{K} \tag{3e}$$

where constraint (3a) enforces the nodal power balance on all DC nodes. Constraint (3b) models the network flow in the lossless HVDC branches, while constraint (3c) models the capacity of the HVDC branches. Constraint (3d) models the lossless power flow across the terminals of converter c, where the power injected into the AC grid has to be withdrawn from the DC grid and vice versa. Constraint (3e) enforces the converter capacity where a_{ck}^{conv} is the contingency mapping of the converter.

2.3. Soft bus-bar splitting

In Fig. 3, a modular converter substation is shown, assuming that it consists of two converter modules. From the AC side, the converter modules can be independently connected to any of the two bus-bar sections of the AC substation. In Fig. 3 (and in the forthcoming sections) we assume these may share a common DC bus, although this need not be the case. Had this converter substation not been modular, there would have been only a single converter module, which can be connected to either of the bus-bar sections (i.e. the two bus-bar sections are isolated upon splitting). This modularity gives rise to what we call "soft bus-bar splitting". As opposed to regular bus-bar splitting, power can now flow indirectly between the two sections in the soft bus-bar splitting setting as the two sections are now connected through a controllable interface (i.e., AC/DC converter modules). In the general case, there can be more than two modules as described in [36], where each module can be connected to one bus-bar section. However, in this work we restrict our studies to only two modules.

In the planning/design phase of such a modular converter substation, it is reasonable (from a reliability perspective) to allocate equal capacities for all of the constituent modules (in case of two modules, then each module would be 50% of the total capacity). During operation, which is the focus of this work, each module can be connected to one bus-bar section, and a converter contingency would mean losing a single converter module. In case of a bipolar HVDC system, the cables can be operated in an unbalanced fashion. This unbalanced operation can be controlled such that the negative and the positive converters are connected to different bus-bar sections, achieving soft bus-bar splitting. To explore the full potential of soft bus-bar splitting, we assume a relaxed version of the converter substation architecture such that: the two converter modules considered are fixed to separate bus-bar sections on the AC side, and the capacity of each module can be continuously

allocated from 0% to 100%. The constraints of the relaxed modular converter substations are:

$$\left\{ 0 \le \gamma_{pk} \le 1, \quad \forall p \in \mathcal{P} \right. \tag{4a}$$

$$|P^{AC}_{ck}|, |P^{DC}_{ck}| \le a^{conv}_{pk} \gamma_{pk} \overline{P_c}, \quad \forall p \in \mathcal{P} \ni c = m^p_1 \tag{4b}$$

$$\left. |P^{AC}_{ck}|, |P^{DC}_{ck}| \le a^{conv}_{pk} (1 - \gamma_{pk}) \overline{P_c}, \quad \forall p \in \mathcal{P} \ni c = m^p_2 \right\}, \forall k \in \mathcal{K} \tag{4c}$$

where p is the index of the modular converter substation. Constraint (4a) enforces the module allocated capacity to be between 0 and 1, which means that if module 1 of converter substation p has 70% of the substation capacity, then module 2 will have 30%. Constraint (4b) enforces the power rating of both the AC and the DC sides of module 1 of the converter pair p, while (4c) is for module 2. a^{conv}_{pk} is the contingency mapping of the modular converter substation.

Finally, as post-contingency converter redispatch can have a cost associated with it, we add the following constraint to keep track of converter power redispatch.

$$\Delta P^{DC}_{ck} \ge |P^{DC}_{ck} - P^{DC}_{c0}| \quad \forall c \in C, \quad \forall k \in \mathcal{K} \setminus \{0\} \tag{5a}$$

2.4. MILP formulation

Model (1) is a mixed-integer linear program (MILP) formulation for security constrained OPF with network topology reconfiguration for hybrid AC/DC grids, where (6a) is the total cost of operation including the cost of corrective actions (i.e., load shedding, curtailment, and converter redispatch). Constraints (6b) enforce the generators capacity limits. Constraint (6c) enforces nodal balance in AC nodes. Constraint (6d) is the power flow physics constraint across an AC transmission line based on the DC approximation, while (6e) enforces the AC transmission line capacities. Constraint (6f) enforces that the load shedding cost (Γ) is at least equal to the worst contingency load shedding, while constraint (6g) limits the load shedding to be at most equal to the demand. Constraint (6i) ensures that no load shedding is taking place pre-contingency.

Model 1. SCOPF-NTR

$$\min_{\delta, \boldsymbol{P}, \boldsymbol{z^r}, \boldsymbol{z^c}, \boldsymbol{LS}, \Gamma} \quad \sum_{g \in \mathcal{G}} C_g P_g + \Gamma \tag{6a}$$

$$\text{s.t.:} \left\{ P^{min}_g \le P_g \le P^{max}_g, \quad \forall g \in \mathcal{G} \right. \tag{6b}$$

$$\sum_{\forall g \in \mathcal{G}_i} (P_g - P^{curt}_{gk}) + \sum_{c \in C_i} P^{AC}_{ck} - \sum_{\forall d \in D_i} (P_d - P^{LS}_{dk}) = \sum_{\forall l \in \mathcal{L} | f_l = i} P_{lk} - \sum_{\forall l \in \mathcal{L} | t_l = i} P_{lk}, \quad \forall i \in \mathcal{N} \tag{6c}$$

$$P_{lk} = a_{lk} B_l (\delta_{f_l k} - \delta_{t_l k}), \quad \forall l \in \mathcal{L} \tag{6d}$$

$$-a_{lk} \overline{P}_l \le P_{lk} \le a_{lk} \overline{P}_l, \quad \forall l \in \mathcal{L} \tag{6e}$$

$$\Gamma \ge \sum_{d \in D} C^{LS} P^{LS}_{dk} + \sum_{g \in \mathcal{G}} C^{curt} P^{curt}_{gk} + \sum_{c \in C} C^{conv} \Delta P^{DC}_{ck} \tag{6f}$$

$$0 \le P^{LS}_{dk} \le P_d, \quad \forall d \in D \tag{6g}$$

$$0 \le P^{curt}_{gk} \le P_g, \quad \forall g \in \mathcal{G} \tag{6h}$$

$$\left. P^{LS}_{d0} = 0, \quad \forall d \in D \right\}, \forall k \in \mathcal{K} \tag{6i}$$

(1), (2), (3), (4), (5) (6j)

2.5. Decomposition to address complexity

To address computational complexity associated with the large number of monitored contingencies in N-1 SCOPF, we develop a decomposition algorithm based on column-and-constraint generation (C&CG) method. In the ith iteration of the C&CG algorithm, we encounter the *master problem*, denoted as **MP**, as described in model 2. **MP** is a simplified form of Model 1 that considers only subset $\mathcal{K}^{(i)}$ contingencies from the full set $\mathcal{K}$. Generally, the size of $\mathcal{K}^{(i)}$ is much smaller than that of $\mathcal{K}$ (i.e., $|\mathcal{K}^{(i)}| \ll |\mathcal{K}|$).

Model 2. **MP**($\mathcal{K}^{(i)}$): Master problem of SCOPF-NTR

$$LB^{(i)} = \min_{\delta, \boldsymbol{P}, \boldsymbol{z^r}, \boldsymbol{z^c}, \boldsymbol{LS}, \Gamma} \quad \sum_{g \in \mathcal{G}} C_g P_g + \Gamma \tag{7a}$$

$$\text{s.t.:} \left\{ (6b) \text{ to } (6j) \right\}, \forall k \in \mathcal{K}^{(i)}$$

The *subproblem*, denoted as **SP** and defined in model 3, treats $\boldsymbol{P_g}$ and $\boldsymbol{z^r}$ as constant values. The purpose of this subproblem is to identify the most critical contingency state, denoted as k, for the input values given of $\boldsymbol{P_g}$ and $\boldsymbol{z^r}$. Consequently, **SP** identifies contingency states that would render the solution found in the previous iteration (i.e., the values of $\boldsymbol{P_g}$ and $\boldsymbol{z^r}$) suboptimal or infeasible. Therefore, such contingency states must be taken into account when formulating the **MP**. The **SP** is formulated as a max–min problem. Furthermore, the inner problem, given by Eqs. (8b)–(8c), is a Mixed-Integer Linear Program (MILP) that models post-contingency actions related to bus-bar splitting and load shedding. Solving the max–min problem is challenging because the standard inner-dualization technique cannot be applied to this type of problems, as noted in [34].

However, the inner problem, represented by Eqs. (8b)–(8c), can be independently solved for each contingency state. In our approach, we leverage parallel computation to solve the inner problem efficiently. Consequently, we calculate ϕ_k, the total imbalance and dispatch costs for each contingency state simultaneously using relatively small MILP problems defined in Eqs. (8b)–(8c). As a result, we solve the maximization problem defined in Eq. (8a) by evaluating the values of ϕ_k. Note that in Eq. (8a) we only consider contingencies that have not been added to the master problem.

Model 3. **SP**($\boldsymbol{z^{r,(i)}}$, $\boldsymbol{P_g}^{(i)}$): Subproblem of SCOPF-NTR

$$UB^{(j)} = \max_{k \in \mathcal{K} \setminus \mathcal{K}^{(i)}} \quad \phi_k \tag{8a}$$

$$\phi_k = \sum C_g \boldsymbol{P_g}^{(i)} + \min_{\delta, \boldsymbol{P}, \boldsymbol{z_c}, \boldsymbol{LS}} \sum_{d \in D} C^{LS} P^{LS}_{dk} + \sum_{g \in \mathcal{G}} C^{curt} P^{curt}_{gk} + \sum_{c \in C} C^{conv} \Delta P^{DC}_{c} \tag{8b}$$

$$\text{s.t.: (6b) to (6j) excluding (6f) and only for contingency } k \tag{8c}$$

The full C&CG algorithm is shown below, where $k = 0$ represents the pre-contingency state (normal state), and ϵ the tolerance gap for stopping the C&CG iterations fixed to 0.1% in our experiments.

3. Case study

We test our proposed methodology on slightly modified versions of IEEE 5, 24, 39, and 67 bus AC/DC benchmark systems that are based

Algorithm 1 C&CG Algorithm

$i \leftarrow 1, \quad \mathcal{K}^{(i)} \leftarrow \{0\}, \epsilon \leftarrow 0.001$
$LB^{(i)} \leftarrow -\infty, \quad UB^{(i)} \leftarrow \infty$
while $\frac{UB^{(i)}-LB^{(i)}}{UB^{(i)}} \geq \epsilon$ **do**
  $LB^{(i+1)}, \boldsymbol{z}^r, \boldsymbol{P_g} \leftarrow$ solve $\mathbf{MP}(\mathcal{K}^{(i)})$
  parfor $k \in \mathcal{K} \setminus \mathcal{K}^{(i)}$ **do**
    $\phi_k \leftarrow$ solve inner $\mathbf{SP}(\boldsymbol{z}^r, \boldsymbol{P_g})$
  end parfor
  $UB^{(i+1)} \leftarrow \max_{k \in \mathcal{K} \setminus \mathcal{K}^{(i)}} \phi_k$
  $\mathcal{K}^{(i+1)} \leftarrow \mathcal{K}^{(i)} \cup \operatorname{argmax}_{k \in \mathcal{K} \setminus \mathcal{K}^{(i)}} \phi_k$
  $i \leftarrow i + 1$
end while

Table 1
Generator data for the 5-bus 2-grid system.

Generator bus	P_{max} (MW)	P_{min} (MW)	C_g ($/MW)
ac 1	250	10	2
ac 2	300	10	3
ac 6	50	10	1
ac 7	100	10	0.5

on *PowerModelsACDC.jl* [9,11]. Modifications were made to reflect system operation under congestion. Modifications made are generally factors multiplied by generator capacities, demand values, and AC transmission lines thermal capacity limits. For the 5-bus 2-grid system we also modify generator costs and capacities as per Table 1 to have asymmetry between the two grids and simulate a net-importing/net-exporting situation, we discuss this in details later. The loading levels range from 75% to 120% of the original nominal loading values with increments of 5%. For the rest of the cases marginal costs of generators and capacities were made a bit more diverse since the original data showed no differentiation between different generators. These systems (24, 39, and 67-bus) were tested in nominal and stressed loading conditions. Nominal refers to original demand values and original transmission capacity limits, and stressed refers to 120% of the demand values and 90% of transmission capacity limits. In all cases generator capacities were multiplied by 130%.

Gurobi (9.0.3) [37] was used as the optimization solver in Julia language [38]. We assume the following values for model parameters: C^{LS}: 1000 $/MW to penalize load shedding as much as possible, C^{curt}: 0 $/MW as curtailment cost is already priced in load shedding cost (because no curtailment occurs without load shedding and vice versa), and C^{conv}: 1 $/MW to incentivize the solver to find topological actions first before resorting to changing converter setpoints. In practice, this change of the setpoint at one end of a DC link will require a change at the other end of the DC link, too, which could involve a cost.

There are several possible combinations of preventive and corrective actions that can be implemented to address system contingencies. We classify our experiments into five categories:

1. **SCOPF (Security-Constrained Optimal Power Flow):** This baseline considers only preventive actions, including generator dispatch and converter set-point adjustments pre-contingency. No topology reconfiguration or converter redispatch is permitted.
2. **NTR (Network Topology Reconfiguration):** This method permits corrective bus-bar splitting and preventive substation reconfiguration. However, converter redispatch is not allowed.
3. **DCC (Dynamic Converter Control):** The only corrective action available under this method is converter redispatch, allowing real-time adjustments to converter outputs during contingencies.
4. **NTRDCC-n (Non-Modular NTR and DCC):** This combines NTR and DCC, allowing both corrective bus-bar splitting and converter redispatch. However, converter modularization is not allowed. This means that when a converter substation is split, the entire converter must be assigned to one of the bus-bar sections without dynamic capacity allocation.
5. **NTRDCC-c (Modular NTR and DCC):** This is the proposed soft bus-bar splitting approach. NTR with soft bus-bar splitting and DCC are allowed. Similar to NTRDCC-n, this method allows both NTR and DCC but introduces modular converter continuous capacity allocation. Upon splitting, the converter can dynamically allocate its capacity to both bus-bar sections simultaneously. Additionally, converter contingencies are also modular, ensuring that only individual modules are affected during a contingency, rather than the entire bulk converter substation.

3.1. Demonstrative example

The 5-bus 2-grid system shown in Fig. 4 is an example of how modern day HVDC technology looks like. This system depicts the popular point-to-point HVDC connections between different zones such as the existing connections between the UK and Norway. We study this system under a monotonically increasing loading level. The aim of this case study is to show case the potential benefits of soft bus-bar splitting.

Fig. 5 presents the operating costs for the 5-bus 2-grid system across the five experimental categories described earlier. Leveraging the two corrective measures: topological actions and dynamic converter set-point adjustments, together consistently achieves lower operating costs compared to relying on either measure individually. Moreover, at higher loading levels, the two measures are necessary to even achieve a feasible system operation. This highlights the complementary nature of these operational flexibility measures, where their combined use effectively enhances system efficiency under contingencies. The highlighted trend in the figure also presents evidence of the benefits of soft bus-bar splitting denoted as NTRDCC-c, as it achieves a 34% less operating cost compared to other corrective measures even in low loading levels where congestion is not imminent yet. This cost reduction is due to the modular property of converters in addition to the ability to achieve asymmetrical operation and dynamically reroute power flows between the two sections of the converter substation. Another highlighted trend is the breakdown of costs, where we can see at nominal operation NTRDCC-c exhibits zero security costs.

Fig. 6 shows the percentage of load shedding at each loading level for the 5-bus 2-grid system. As shown in the figure, point *a* (circled) highlights the last feasible loading level for SCOPF and DCC, both exhibiting the same amount of load shedding. Point *b* shows the highest feasible loading level for NTR. Also, when seen in light of the full profile of NTR, point *b* shows that above some loading level (115% in that case), post-contingency load shedding cannot result in a secure operation; this can be inferred from the slope of NTR right before point *b*, where the rate of load shedding is much smaller than the subsequent rate of load shedding between 105% to 110% loading. The significant change of load shedding values for NTR between loading levels 105% and 110% indicates a change of regime (i.e., new binding constraints) in the OPF solution. This change in regime suggests that the system is too stressed to handle the increase in the loading level. This stressed state of the system leads the solver to only find feasible solutions by increasing load shedding. The study demonstrates that the combination of topology reconfiguration and dynamic converter control leads to less load shedding than any of the measures individually.

Fig. 7 shows the maximum amount of post-contingency converter redispatch needed at each loading level. While for SCOPF and NTR post-contingency converter redispatch is always zero by definition, for NTRDCC-c (soft bus-bar splitting) converter redispatch was not needed to achieve optimal operation. NTRDCC-c poses no converter redispatch needs as for this test case, the worst contingency is always a converter contingency. NTRDCC-c eliminates the effect of converter contingencies by virtue of modular converter architecture, where if a module fails, the power can still be transmitted through the other module (i.e., we assume no single point of failure). The key insight here is that the

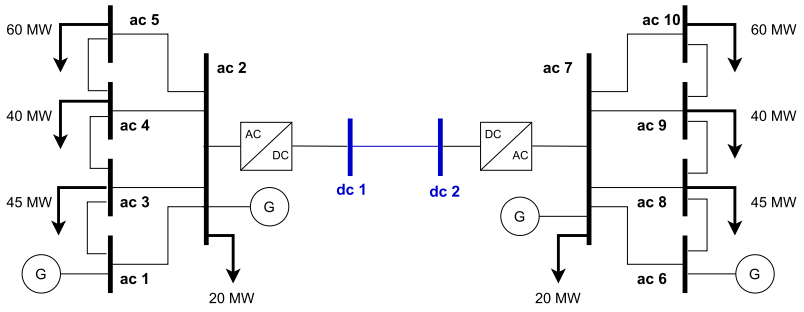

Fig. 4. 5-bus 2-grid case study.

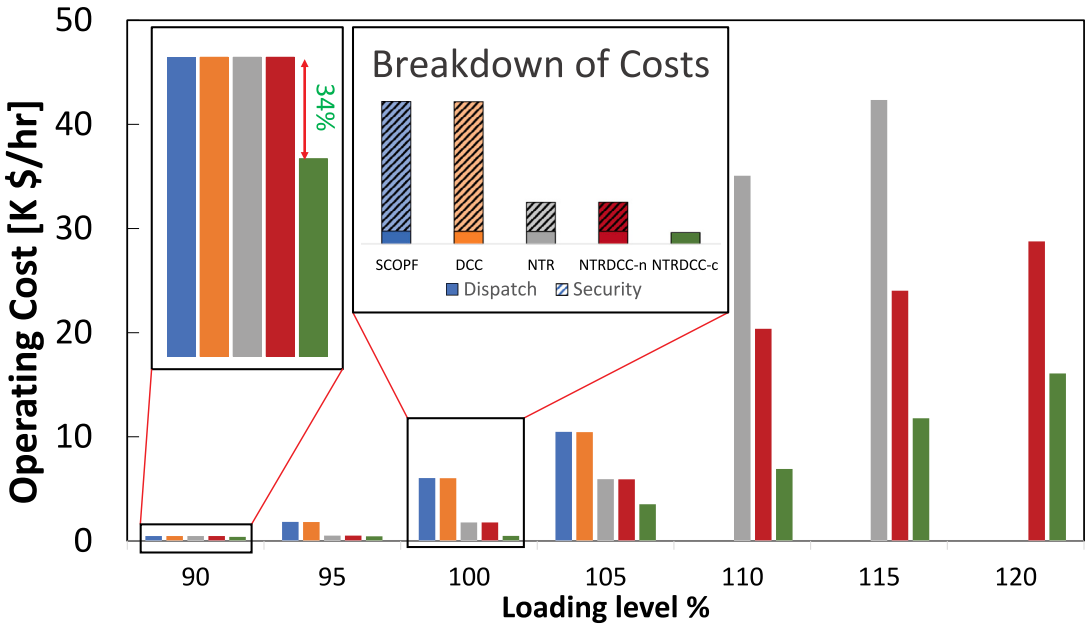

Fig. 5. Operating costs at different loading levels for the 5-bus 2-grid system. SCOPF DCC NTR NTRDCC-n NTRDCC-c.

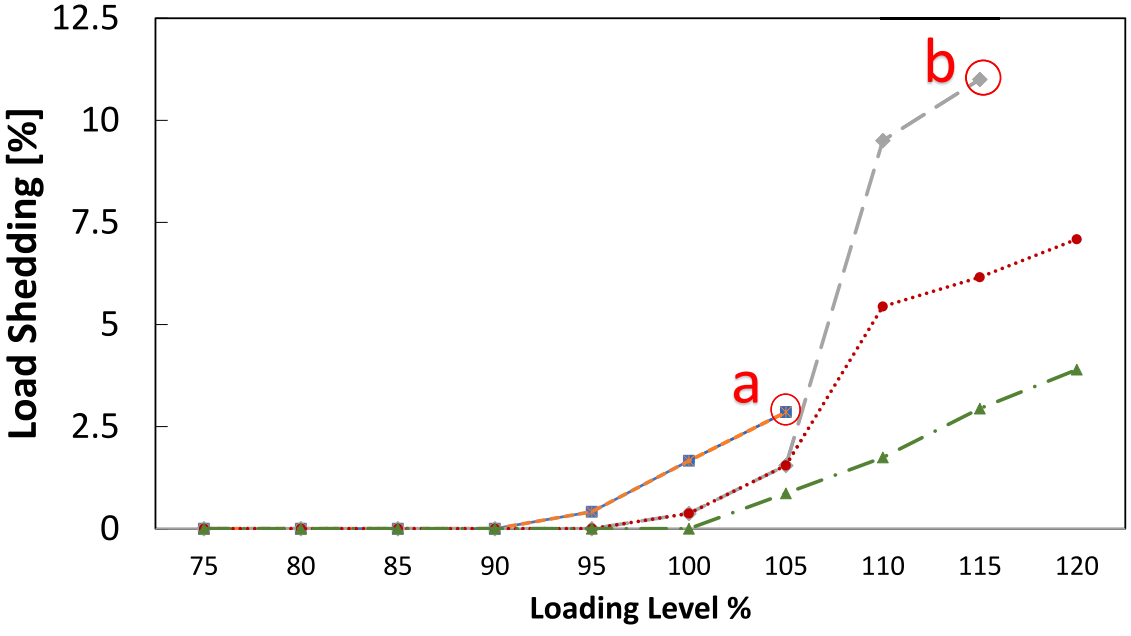

Fig. 6. Load shedding for the 5-bus 2-grid system at different loading levels. SCOPF DCC NTR NTRDCC-n NTRDCC-c.

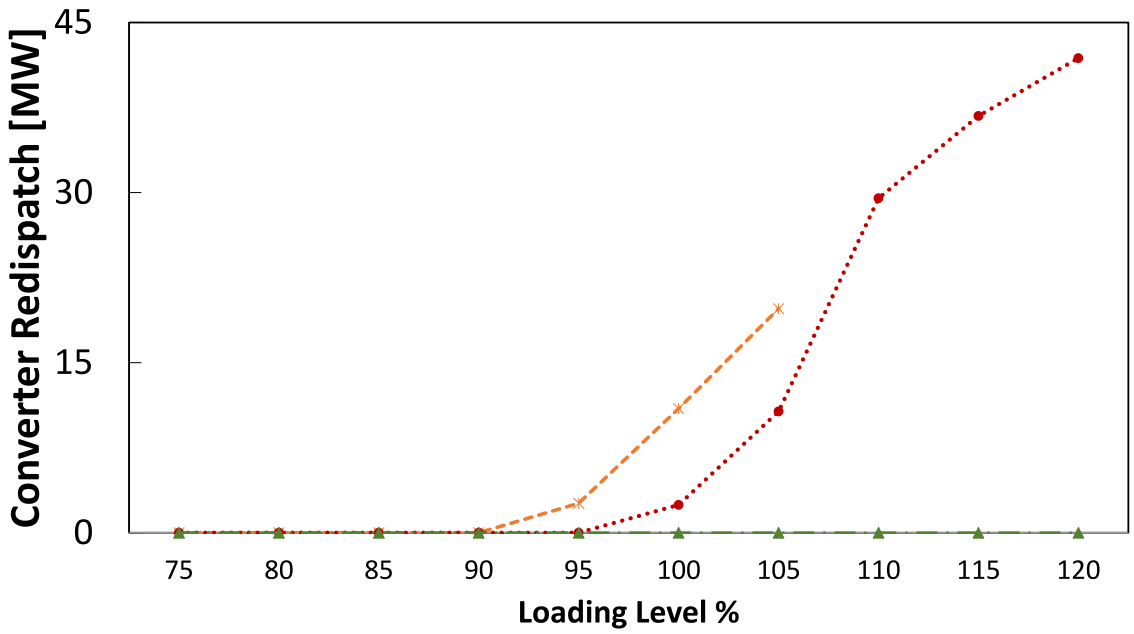

Fig. 7. Converter redispatch needs for the 5-bus 2-grid system. DCC NTRDCC-n NTRDCC-c.

utilization of both NTR and DCC simultaneously leads to less converter redispatch needs. This insight is particularly important as this case study could be thought of as two independent grids connected via a back-to-back converter-based link. The security of the power-importing grid depends on whether the operator on other end of the HVDC link is capable/willing to change the converter set-points (i.e, redispatch converters), but introducing soft bus-bar splitting leads to less need for that redispatch of converters.

3.2. Impact assessment on larger systems

This case study investigates the impact of the five experimental categories/methods on systems larger than the 5-bus 2-grid system used for demonstration (i.e., 24, 39, and 67-bus systems). We assess the impact of each method based on three criteria: economic costs, security, and converter redispatch needs. We also show the computational time taken for the CCG decomposition to solve the resulting MILP models of the case studies. Fig. 8 is an exhibition of the results for the aforementioned systems.

3.2.1. Economic costs

Fig. 8(a) to 8(c) present the normalized operating costs for the 24, 39, and 67-bus systems respectively. All costs are normalized with respect to SCOPF baseline cost. The key trend again is that the combination of both network topology reconfiguration and post-contingency converter redispatch yields the lowest operating costs. In the 24 and 39-bus systems the introduction of NTR alone results in similar operating costs compared to the NTRDCC variants. However, for the 67-bus system this is not the case. Fig. 8(c) shows that DCC resulted in a lower operating cost compared to NTR under nominal operating conditions, while in stressed conditions, NTR and SCOPF were infeasible (hence costs are normalized with respect to DCC). The normalized cost associated with the proposed soft bus-bar splitting is the lowest. These observations demonstrate the superiority of NTRDCC approaches in maximizing the grid utilization.

3.2.2. Security

Security of operation, quantified by percentage of load shedding (out of the total load) at the worst contingency, is also enhanced through the application of NTRDCC variants as shown in Fig. 8(d) to 8(f). Figs. 8(d) and 8(e) show that corrective topological actions can improve operational security. Fig. 8(f) demonstrate the significant security enhancement provided by the introduced soft bus-bar splitting (NTRDCC-c), where the need for load shedding post-contingency is eliminated.

3.2.3. Converter redispatch

Similarly with post-contingency converter redispatch shown in Fig. 8(g) to 8(i), less power is rerouted through the converters when NTR is used. We note that, for the 39-bus system, the post-contingency converter redispatch at the worst contingency for DCC decreases in the stressed operating conditions as shown in Fig. 8(h), as opposed to what happens for the 24 and 67-bus systems shown in Fig. 8(g), and 8(i). This highlights that at different operating conditions the worst contingency change, as a result, the optimal corrective actions will change (i.e., in this case we observe that load shedding increases to accommodate for the worst contingency when the system operates under stressed operating conditions). These observations evidently show that less converter redispatch is needed when NTRDCC variants are used.

3.2.4. Computational time

Fig. 9 shows the computational time taken to solve each of the 24, 39, and 67-bus systems under stressed operating conditions using the CCG algorithm. Solving the same problems without decomposition for the 3 systems did not produce acceptable solutions (MIPGap > 7% on average) within 60 min of solving, thus, simulations were terminated. It is worth noting that the stressed 39-bus system takes more time than the 67-bus system, which suggests that the complexity of the problem is not only subject to the size of the system, but also to the grid connectivity and the location of the congestion that is addressed by switching maneuvers. For example, a substation that injects power into the grid and has six transmission lines connected, one of which is congested, may be easier to solve than a substation with only four transmission lines, as there are more options to reroute the power flows. However, such relationships become increasingly complex to reason when switchable substations are a few nodes away from congested lines.

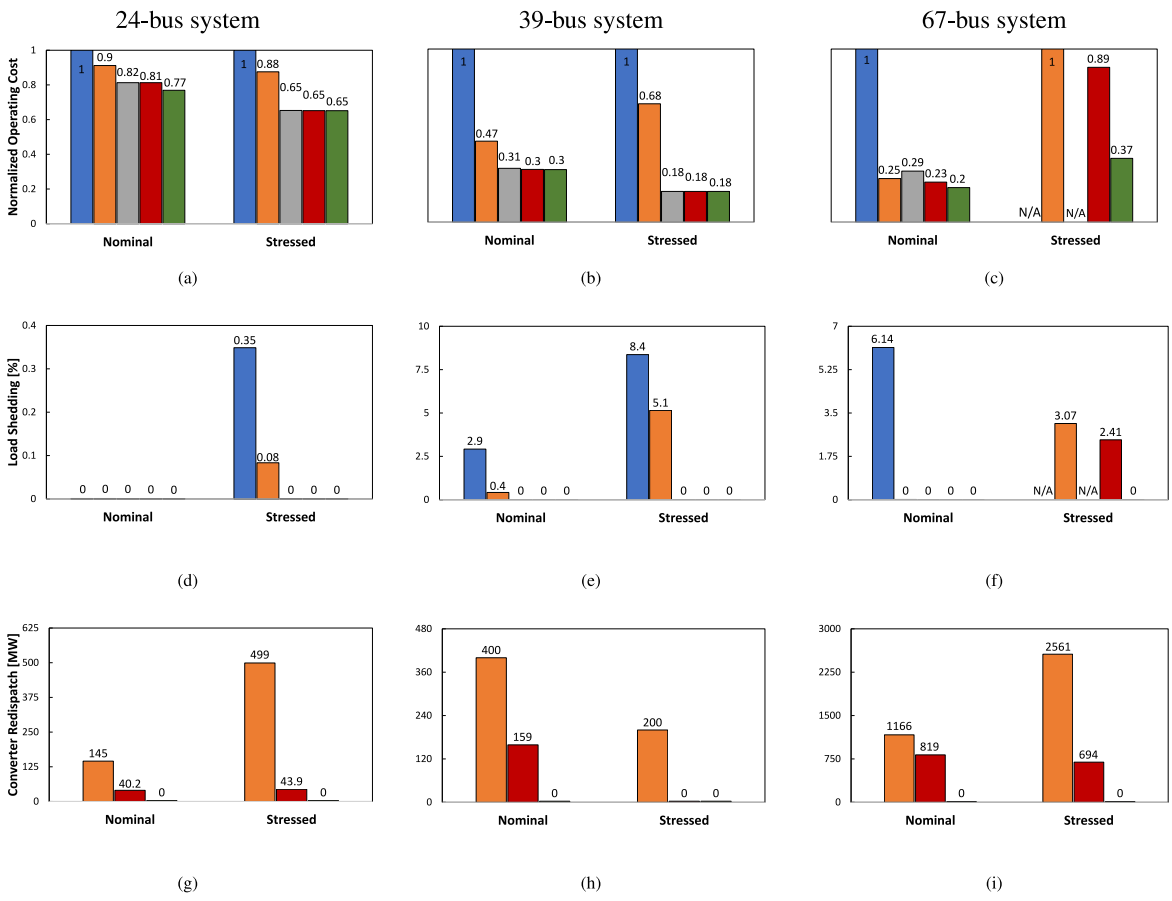

Fig. 8. Comparison of the proposed method across three categories (rows: Normalized Cost, Load Shedding, and Converter Redispatch) and three cases (columns: 24-bus, 39-bus, and 67-bus systems). SCOPF DCC NTR NTRDCC-n NTRDCC-c.

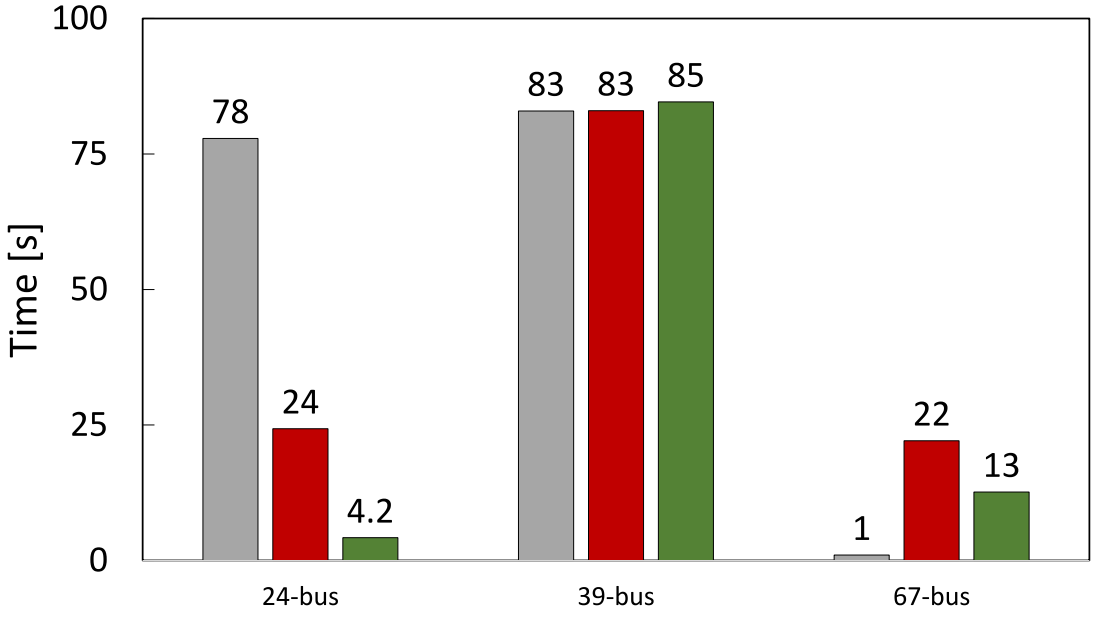

Fig. 9. Computational time for stressed operating conditions. NTR NTRDCC-n NTRDCC-c.

4. Discussion

This paper demonstrates that the proposed method of combining corrective post-contingency converter redispatch and soft bus-bar splitting significantly reduces the operating costs and improves system security. These improvements are direct results of the extra operational flexibility granted by the utilization of the extra degrees of freedom of network topology reconfiguration. Even without soft bus-bar splitting, we observe considerable improvements in operating costs and security with the combination of post-contingency converter control (DCC) and network topology reconfiguration (NTR).

The authors are not previously aware of a proposed HVDC converter architecture that operates in the way proposed with soft bus-bar splitting (with continuous capacity allocation to modules). Future works should therefore consider the control and cost implications of the use of converters in this modular fashion (as compared to construction via a single monolithic converter). Nevertheless, there are other ways that controllable HVDC links might be operated in a similar way, albeit without a shared DC link. When HVDC systems are operated in a bipolar fashion with appropriate current return path, it can be possible to operate the cable in an unbalanced sense, i.e., positive and negative AC/DC converters of the link transferring different amounts of power [39,40]. In such a system, the positive and negative converters could then be connected to different AC buses. Alternatively, if there are multiple wind farms or HVDC links whose own individual HVDC converter stations interface with the transmission system at the same substation, these could each be independently controlled on each bus.

5. Conclusion

We conclude that applying NTR through substation reconfiguration and bus-bar splitting in hybrid AC/DC grids reduces the operating cost significantly as compared to both preventive SCOPF and SCOPF with only corrective converter redispatch. Furthermore, the benefits of modular architectures of converter substations can be fully exploited with soft bus-bar splitting since the converter modules can inject/absorb power to/from two electrical nodes instead of only one, which means additional degrees of freedom for rerouting the power flows. We also conclude that a modular converter substation will result in less need for post-contingency converter redispatch. Finally, the incorporation of corrective topological actions along side with converter redispatch show great potential for maximizing grid capacity utilization.

Future work is needed on modeling the physics of both AC and DC grids more accurately using the actual non-linear models or a convex relaxation. In this paper, we only assumed topological actions in the AC side, however, this could also be extended to the DC grid. Although power flow is highly controllable in the DC side, yet in a meshed DC grid topology reconfiguration can introduce even more flexibility.

CRediT authorship contribution statement

Basel Morsy: Writing – original draft, Visualization, Software, Methodology, Investigation, Data curation, Conceptualization. **Matthew Deakin:** Writing – review & editing, Writing – original draft, Resources, Methodology, Conceptualization. **Adolfo Anta:** Writing – review & editing, Resources, Conceptualization. **Jochen Cremer:** Writing – review & editing, Supervision.

Declaration of competing interest

The authors declare that they have no known competing financial interests or personal relationships that could have appeared to influence the work reported in this paper.

Data availability

Data will be made available on request.

References

[1] European Commission. 2050 long-term strategy: A clean planet for all. 2018, URL https://climate.ec.europa.eu/eu-action/climate-strategies-targets/2050-long-term-strategy_en, Accessed [insert date here].

[2] Agency for the Cooperation of Energy Regulators (ACER). ACER Market Monitoring Report 2024: Cross-zonal Electricity Trade Capacities. 2024, URL https://www.acer.europa.eu/monitoring/MMR/crosszonal_electricity_trade_capacities_2024, Accessed [December 2024].

[3] ENTSO-E. Position paper on improving HVDC system reliability. 2018, [Online]. Available: https://entsoe.eu/2018/12/10/improving-hvdc-system-reliability/.

[4] Van Hertem D, Ghandhari M. Multi-terminal VSC HVDC for the European supergrid: Obstacles. Renew Sustain Energy Rev 2010;14(9):3156–63. http://dx.doi.org/10.1016/j.rser.2010.07.068.

[5] Pierri E, Binder O, Hemdan NGA, Kurrat M. Challenges and opportunities for a European HVDC grid. Renew Sustain Energy Rev 2017;70:427–56. http://dx.doi.org/10.1016/j.rser.2016.11.233.

[6] Barnes M, Van Hertem D, Teeuwsen SP, Callavik M. HVDC systems in smart grids. Proc IEEE 2017;(11). http://dx.doi.org/10.1109/JPROC.2017.2672879.

[7] Wang M, An T, Ergun H, Lan Y, Andersen B, Szechtman M, Leterme W, Beerten J, Van Hertem D. Review and outlook of HVDC grids as backbone of transmission system. CSEE J Power Energy Syst 2021;7(4):797–810. http://dx.doi.org/10.17775/CSEEJPES.2020.04890.

[8] (IRENA) IREA. Virtual power lines. Innovation landscape brief. 2020, URL https://www.irena.org/-/media/Files/IRENA/Agency/Publication/2020/Jul/IRENA_Virtual_power_lines_2020.pdf.

[9] Ergun H, Dave J, Van Hertem D, Geth F. Optimal Power Flow for AC–DC grids: Formulation, convex relaxation, linear approximation, and implementation. IEEE Trans Power Syst 2019;34. http://dx.doi.org/10.1109/TPWRS.2019.2897835.

[10] Saplamidis V, Wiget R, Andersson G. Security constrained Optimal Power Flow for mixed AC and multi-terminal HVDC grids. In: 2015 IEEE eindhoven PowerTech. 2015, p. 1–6. http://dx.doi.org/10.1109/PTC.2015.7232616.

[11] Bhardwaj V, Ergun H, Van Hertem D. Risk-based preventive-corrective security constrained optimal power flow for AC/DC grid. In: 2021 IEEE madrid PowerTech. 2021, p. 1–6. http://dx.doi.org/10.1109/PowerTech46648.2021.9495030.

[12] contributors W. List of HVDC projects *Wikipedia* n.d.. URL https://en.wikipedia.org/wiki/List_of_HVDC_projects.

[13] Bacher R, Glavitsch H. Network topology optimization with security constraints. IEEE Trans Power Syst 1986;103–11.

[14] Schnyder G, Glavitsch H. Integrated security control using an Optimal Power Flow and switching concepts. IEEE Trans Power Syst 1988;3(2):782–90. http://dx.doi.org/10.1109/59.192935.

[15] Schnyder G, Glavitsch H. Security enhancement using an optimal switching power flow. In: Conference papers power industry computer application conference. 1989, p. 25–32. http://dx.doi.org/10.1109/PICA.1989.38970.

[16] Fisher EB, O'Neill RP, Ferris MC. Optimal transmission switching. IEEE Trans Power Syst 2008;23(3):1346–55. http://dx.doi.org/10.1109/TPWRS.2008.922256.

[17] Hedman KW, O'Neill RP, Fisher EB, Oren SS. Optimal transmission switching with contingency analysis. IEEE Trans Power Syst 2009;24(3):1577–86. http://dx.doi.org/10.1109/TPWRS.2009.2020530.

[18] Hedman KW, Ferris MC, O'Neill RP, Fisher EB, Oren SS. Co-Optimization of generation unit commitment and transmission switching with N-1 reliability. IEEE Trans Power Syst 2010;25(2):1052–63. http://dx.doi.org/10.1109/TPWRS.2009.2037232.

[19] Khodaei A, Shahidehpour M. Transmission switching in security-constrained unit commitment. IEEE Trans Power Syst 2010;25(4):1937–45. http://dx.doi.org/10.1109/TPWRS.2010.2046344.

[20] Barrows C, Blumsack S, Bent R. Computationally efficient optimal Transmission Switching: Solution space reduction. In: 2012 IEEE power and energy society general meeting. 2012.

[21] Heidarifar M, Doostizadeh M, Ghasemi H. Optimal transmission reconfiguration through line switching and bus splitting. In: 2014 IEEE PES general meeting | conference & exposition. 2014.

[22] Trodden PA, Bukhsh WA, Grothey A, McKinnon KIM. MILP islanding of power networks by bus splitting. In: 2012 IEEE power and energy society general meeting. p. 1–8. http://dx.doi.org/10.1109/PESGM.2012.6345046.

[23] Heidarifar M, Ghasemi H. A network topology optimization model based on substation and node-breaker modeling. IEEE Trans Power Syst 2016;31(1):247–55. http://dx.doi.org/10.1109/TPWRS.2015.2399473.

[24] Goldis EA, Ruiz PA, Caramanis MC, Li X, Philbrick CR, Rudkevich AM. Shift factor-based SCOPF Topology Control MIP formulations with substation configurations. IEEE Trans Power Syst 2017;32(2):1179–90. http://dx.doi.org/10.1109/TPWRS.2016.2574324.

[25] Morsy B, Hinneck A, Pozo D, Bialek J. Security constrained OPF utilizing substation reconfiguration and busbar splitting. Electr Power Syst Res 2022.
[26] Dabbaghjamanesh M, Moeini A, Hatziargyriou ND, Zhang J. Deep learning-based real-time switching of hybrid AC/DC transmission networks. IEEE Trans Smart Grid 2021;12(3):2331–42. http://dx.doi.org/10.1109/TSG.2020.3041853.
[27] Zhu L, Rong X, Zhao J, Zhang H, Zhang H, Jia C, Ma G. Topology optimization of AC/DC hybrid distribution network with energy router based on power flow calculation. Energy Rep 2022;8:1622–38. http://dx.doi.org/10.1016/j.egyr.2022.02.208, 2021 International Conference on New Energy and Power Engineering. URL https://www.sciencedirect.com/science/article/pii/S2352484722004553.
[28] Bastianel G, Vanin M, Hertem DV, Ergun H. Optimal transmission switching and busbar splitting in hybrid AC/DC grids. 2024, arXiv:2412.00270. URL https://arxiv.org/abs/2412.00270.
[29] Shi H, Ding L, Chen G, Shi P, Liu T, Liu H. Network topology optimization for hybrid AC DC power grid based on critical node identification and busbar switching. In: 2024 9th Asia conference on power and electrical engineering. ACPEE, 2024, p. 72–6. http://dx.doi.org/10.1109/ACPEE60788.2024.10532381.
[30] European Commission. Implementation plan on "High Voltage Direct Current (HVDC) and DC Technologies". 2021, https://setis.ec.europa.eu/system/files/2022-02/SETPlan_HVDC_DC_Tech_ImplementationPlan_Final.pdf, [Accessed 28 September 2023].
[31] Lehmann K, Grastien A, Hentenryck PV. The complexity of DC-switching problems. Tech. rep., NICTA; 2014.
[32] Bouffard F, Galiana F, Arroyo J. Umbrella contingencies in security-constrained Optimal Power Flow. 2005.
[33] Ardakani AJ, Bouffard F. Identification of umbrella constraints in DC-Based security-constrained optimal power flow. IEEE Trans Power Syst 2013.
[34] Zeng B, Zhao L. Solving two-stage robust optimization problems using a column-and-constraint generation method. Oper Res Lett 2013.
[35] Hinneck A, Morsy B, Pozo D, Bialek J. Optimal power flow with substation reconfiguration. In: IEEE PowerTech. 2021, p. 1–6. http://dx.doi.org/10.1109/PowerTech46648.2021.9494797.
[36] Gkountaras A, Strafiel C, Buschmeyer T, Bartsch M. Modularity of grid inverters in modern power systems. In: Power electronic components and their applications 2017; 7. ETG-symposium. 2017, p. 1–7.
[37] Gurobi Optimization L. Gurobi optimizer reference manual. 2021, URL https://www.gurobi.com.
[38] Bezanson J, Edelman A, Karpinski S, Shah VB. Julia: A fresh approach to numerical computing. SIAM R Eview 2017.
[39] Leterme W, Tielens P, De Boeck S, Van Hertem D. Overview of grounding and configuration options for meshed HVDC grids. IEEE Trans Power Deliv 2014;29(6):2467–75.
[40] Jat CK, Bhardwaj V, Ergun H, Van Hertem D. Security constrained OPF model for AC/DC grids with unbalanced DC systems. IET 2023.